

A finite element approach for the continuum spectrum of the Dirac radial equation

L.A.A. Nikolopoulos

*Department of Telecommunication Science and Technology, University of Peloponnese,
GR-221 00, Tripolis, Greece*

E-mail: nlambros@uop.gr

Received 17 September 2004

The Dirac radial functions are expanded in polynomial B-spline basis, transforming the Dirac equation in a generalized eigensystem matrix problem. Due to the locality nature of the B-spline functions the matrix representation of all the involved operators are highly sparse. Diagonalization of the matrix equations provides the bound and continuum eigenstates. Energies and oscillator strengths for Hydrogen and Rubidium are presented.

KEY WORDS: Dirac equation, B splines, photoionization

AMS subject classification: 65705, 81V05

1. Introduction

In our days, ultra-intense femtosecond infrared laser pulses can be produced in laboratories, rather easily. Peak intensities of the order 10^{20} W/cm², are reached with some effort. Free electrons in an electromagnetic field (EMF) performs an oscillatory motion, where the kinetic energy, named ponderomotive energy U_p , is a measure of the strength of the interaction with the EMF. When the ponderomotive energy approaches the rest energy of the electron $m_e c^2$ the theoretical treatment of the interaction process should be made relativistically, since the velocity of the electrons is regarded relativistic. Generation of strong extreme ultraviolet (xuv) laser pulses with durations within the femtosecond range has become feasible during the development of the free electron laser (FEL) at DESY [1]. At the same time, table-top high-order harmonic generation (HOHG) from Ti:sapphire femtosecond lasers have been proven to be able to produce non-linear processes when interacting with atomic systems [2–4]. Radiation with these properties, offer the possibility for the exploration of highly charged ions [5] as well as the excitation and ionization of electrons belonging to inner-shell states of heavy atomic systems.

The rapid evolution of the attosecond technology, among others, has provided the experimental tool for performing inner-shell spectroscopy of

core-excited atoms, since the characteristic time constants of the relevant dynamics range from femtosecond to few attoseconds [6]. Finally, the importance of the spin-orbit coupling, a purely relativistic phenomenon, grows as the atomic number Z increases [7,8].

Inspired by the pioneer work by Johnson et al. [9], we expand the Dirac radial equation in a finite basis set, such as the B-spline polynomials [10], transforming the equations into a generalized matrix eigenvalue problem, solved by standard diagonalization techniques. Careful normalization of the discrete states (both bound and continuum) is taken place, in order to be able to produce dipole matrix elements, oscillator strengths as well ionization cross sections.

First, we give the basic definitions and equations for the relativistic treatment of atomic systems. In addition, formulas for the calculation of the matrix elements (dipole allowed) and oscillator strengths between Dirac states are given. Then we apply the finite basis (B-splines) to the Dirac radial equation for an electron in a central potential $U(r)$ and derive the matrix equations. And finally, we discuss specific choices for the central potential. For example, for hydrogenic systems the potential is the pure coulombing potential ($U(r) = -Z/r$, Z the atomic number) while for one-electron valence atomic systems (i.e. Rb, Cs,..) we have chosen to implement two different potentials, taken from the literature. Atomic units ($\hbar = m_e = e = 1$) used through out the text.

2. Theoretical background

The field-free Dirac Hamiltonian is of the type:

$$H_D = c\boldsymbol{\alpha} \cdot \mathbf{p} + \beta c^2 + U(r) \quad \alpha = \begin{bmatrix} 0 & \sigma \\ \sigma & 0 \end{bmatrix}, \quad \beta = \begin{bmatrix} 1 & 0 \\ 0 & -1 \end{bmatrix}, \quad (1)$$

where σ and $\mathbf{1}$ are the 2×2 Pauli and the diagonal matrices, respectively. The central potential is given by $U(r) = -Ze^2/r + V_l(r)$, with $-Ze^2/r$ being the nuclear potential and $V_l(r)$ the ‘screening’ potential which is either a model potential or a Dirac–Fock potential determined self-consistently.

Straightforward partial wave analysis gives for the time-independent radial Dirac equation in a central potential:

$$h_D(r)P_\varepsilon(r) = \varepsilon P_\varepsilon(r), \quad P(r) = \begin{bmatrix} G(r) \\ F(r) \end{bmatrix} \quad (2)$$

with $\varepsilon = E - mc^2$ the ‘transformed’ energy and h_D given by:

$$h_D(r) = \begin{bmatrix} U(r) & c\left(-\frac{d}{dr} + \frac{k}{r}\right) \\ c\left(\frac{d}{dr} + \frac{k}{r}\right) & -2c^2 + U(r) \end{bmatrix} \quad (3)$$

with the quantum number k being the relativistic analog of the l quantum number in the classification of the states in the Schrödinger equation (SE). Knowledge of k is equivalent to knowledge of the quantum numbers j, l of the j^2, l^2 operators.

2.1. Relativistic dipole matrix elements

In photoionization studies the accurate determination of the dipole matrix elements $\langle \phi_f | \mathbf{D} | \phi_i \rangle$ and the eigenenergies $\varepsilon_f, \varepsilon_i$, for each pair of the eigenfunctions $\phi_i(r), \phi_f(r)$, are of essential importance. For one-electron atoms, the non-relativistic dipole operator is $\mathbf{D} = -i\nabla = \mathbf{p}$, where \mathbf{p} is the momentum operator of the valence electron. Elementary operator algebra gives the relation $\langle \phi_i | \mathbf{p} | \phi_f \rangle = i(\varepsilon_i - \varepsilon_f) \langle \phi_i | \mathbf{r} | \phi_f \rangle$, thus providing an equivalent form for the dipole matrix elements.

In the relativistic case the eigenstates are spinor states $\psi_i(r), \psi_f(r)$, characterized by the quantum numbers $(n, j, l, m_j) \equiv (n, k, m_j)$. The relativistic transition matrix element between the states ψ_i, ψ_f , assuming photons of energy $\omega = ck$, polarization vector \hat{e}_k and in the *long-wavelength* ($e^{i\mathbf{k}\cdot\mathbf{r}} \sim 1$) approximation (or dipole approximation) is given by [11]:

$$D_{fi}^{(g)}(\mu) = i\sqrt{\frac{\omega}{2c}} \hat{e}_k \cdot \mathbf{D}_{fi}^{(g)}(\mu) = (-1)^{j_f - m_f} \begin{bmatrix} j_f & 1 & j_i \\ -m_f & \mu & m_i \end{bmatrix} \langle f || D || i \rangle, \quad (4)$$

where $\mu = 0, \pm 1$ denotes the spherical components of the dipole operator $\mathbf{D}^{(g)}$, $g = l, v$, given by:

$$\mathbf{D}^{(g)} = \begin{cases} -ic\alpha, & g = v, \text{ velocity gauge,} \\ \mathbf{r}, & g = l, \text{ length gauge.} \end{cases}$$

The reduced matrix element $d_{fi} = \langle f || D || i \rangle$, is expressed as a product of an angular factor and a radial integral, namely:

$$\begin{aligned} d_{fi}^{(g)} &= \delta_{l_f l_i} (-1)^{j_f + 1/2} \sqrt{(2j_f + 1)(2j_i + 1)} \begin{bmatrix} j_f & j_i & 1 \\ -\frac{1}{2} & \frac{1}{2} & 0 \end{bmatrix} R_{fi}^{(g)}, \\ R_{fi}^{(l)} &= \int_0^R dr r [G_f(r)G_i(r) + F_f(r)F_i(r)], \\ R_{fi}^{(v)} &= \int_0^R dr [(k_f - k_i - 1)G_f(r)F_i(r) + (k_f - k_i + 1)G_i(r)F_f(r)]. \end{aligned}$$

The partial and the multiplet oscillator strengths for a transition between the states $i \equiv (n, l)$, $f = (n, l + 1)$ for one-electron atoms are given by:

$$f(nlj \rightarrow n, l + 1, j) = \frac{2\omega}{3} \frac{1}{4j(j+1)} |R(nlj; n, l + 1, j)|^2, \quad (5)$$

$$f(nlj \rightarrow n, l + 1, j + 1) = \frac{2\omega}{3} \frac{2j + 3}{4(j + 1)} |R(nlj; nl + 1j + 1)|^2, \quad (6)$$

$$f(nl \rightarrow nl + 1) = \frac{2\omega}{3} \frac{l + 1}{4(2l + 1)} |R(nl; nl + 1)|^2. \quad (7)$$

3. Dirac equation and B-splines basis

3.1. Eigenenergies and radial eigenstates

Detailed presentation and application of the method has been given by Johnson and Sapirstein in a pioneering paper [9]. However, attention has been given mainly for the bound state of the atomic systems. Here we present a method, which is capable to represent the continuum relativistic states at high accuracy.

The basic idea is the same as in the non-relativistic case, which is the confinement of the atom in a sphere (box) of radius R . This has the effect of the finiteness of the number of the bound states (for $R \rightarrow \infty$ this number is infinite) and the discretization of the continuum spectrum, while the number of the continuum states remains infinite. The equations to be solved, are derived using the action principle, which has the advantage of introducing the boundary condition into the radial equations in a systematical manner.

Expanding the radial functions in a B-spline set of order k_s , total number n_s , defined in a region $[0, R]$, [10] as:

$$G_k(r) = \sum_{i=1}^{n_s} p_i^{(k)} B_i(r), \quad F_k(r) = \sum_{i=1}^{n_s} q_i^{(k)} B_i(r), \quad (8)$$

we obtain the $2n_s \times 2n_s$ generalized eigenvalue equation, from $\partial S / \partial p_i = 0$, $\partial S / \partial q_i = 0$:

$$\begin{aligned} \mathbf{A} \cdot \mathbf{u}^{(k)} &= \varepsilon_k \mathbf{B} \cdot \mathbf{u}^{(k)}, \\ \mathbf{u}^{(k)} &= (p_1^k, p_2^k, \dots, p_{n_s}^k, q_1^k, q_2^k, \dots, q_{n_s}^k), \end{aligned} \quad (9)$$

where the A, B matrices are given by:

$$A = \begin{bmatrix} \mathbf{M}(U) & c\mathbf{M} \left(\frac{d}{dr} - \frac{k}{r} \right) \\ -c\mathbf{M} \left(\frac{d}{dr} + \frac{k}{r} \right) & -2c^2\mathbf{M}(1) + \mathbf{M}(U) \end{bmatrix} + A_S(R) \quad (10)$$

and

$$B = \begin{bmatrix} M(1) & 0 \\ 0 & M(1) \end{bmatrix}. \quad (11)$$

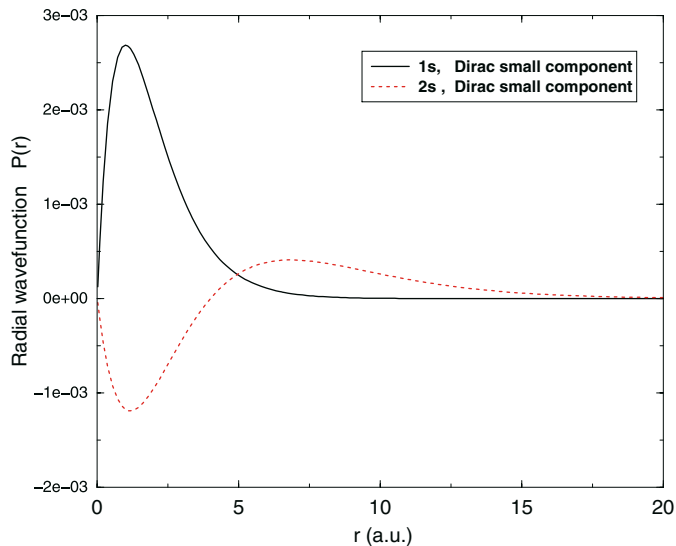


Figure 1. Hydrogen relativistic radial bound states. The B-splines parameters were $n_s = 100, k_s = 9, R = 100$ a.u. and the knotpoint distribution was linear-like.

The elements of the matrix M are given by the integral $M_{ij}(q) = \int_0^R B_i(r)q(r)B_j(r)$. The elements of the “boundary” matrix $A_S(R)$ are derived from the variational equations, $\partial S_b/\partial p_i = 0, \partial S/\partial q_i = 0$. The solution of the above system gives n_s states with $\varepsilon > 0$ (positive states) and n_s states with $\varepsilon < 0$ (negative states). As an representative example in figure 1 we plot the small and large components of the $1s, 2s$ radial functions of hydrogen. In table 1 we show eigenenergies of the ns states of the Hydrogen, obtained with the Dirac Hamiltonian H_D analytically and numerically.

Table 1
Energies of the ns states of the Hydrogen, obtained with the Dirac Hamiltonian H_D analytically and numerically. The B-splines parameter are $k_s = 9, n_s = 200, R = 200$ a.u. and linear grid.

$ns_{1/2}$	ω_n	
	Analytical	B-splines
1	-0.50000665656957	-0.50000665656997
2	-0.12500208019145	-0.12500208018833
3	-0.055556295171932	-0.05555629517705
4	-0.031250338036512	-0.031250338031454
5	-0.020000181052151	-0.020000181060167
6	-0.01388899674244	-0.013888996751446
7	-0.010204150879325	-0.010204150944494

3.2. Continuum states and normalization

In atomic quantum theory, bound states are normalized to unity while the continuum eigenstates are energy normalizable. Leaving the angular part normalization out of the discussion we have for the radial part of the wavefunction $\langle P_a | P_b \rangle = \delta_{ab}$. The physical meaning of the calculated positive-energy wavefunctions $\bar{P}_{\varepsilon_i}(r)$ within the basis-set framework is the following: The positive-energy solutions $\bar{P}_{\varepsilon_i}(r)$ (normalized in unity), when divided by the weight w_i which allows integration over the continuum, represent the actual continuum Coulomb function, of energy ε_i , inside the box.

$$P_{\varepsilon_i}(r) = A_i \bar{P}_{\varepsilon_i}(r), \quad r < R. \quad (12)$$

The adoption of boundary conditions at finite radius determines the spacing of consecutive energy eigenvalues, or equivalently the density of states. The density of states $\rho(E)$ instead of the δ -function form takes now finite values, $\rho(E_i) = 2/(E_{i+1} - E_{i-1})$. Choosing as normalization factor the square inverse of the density of energy, namely, $A_i = \frac{1}{\sqrt{\rho(\varepsilon_i)}} = \sqrt{\frac{2}{\varepsilon_{i+1} - \varepsilon_{i-1}}}$ for the normalization of the discrete positive-energy states we obtain, $\langle P_i | P_j \rangle = \rho(\varepsilon_i) \xrightarrow{R \rightarrow \infty} \delta(\varepsilon_i - \varepsilon_j)$. The limit of this finite normalization when $R \rightarrow \infty$ goes to δ -function as it should.

3.3. Hydrogenic atomic systems, Finite-size nucleus

The hydrogenic Dirac wavefunctions for $j = 1/2$ diverges near the origin $r \rightarrow 0$, in contrast to those of the hydrogenic Schrödinger wavefunctions, which remains finite for $l = 0$. Although the divergence is quite weak, it becomes more serious when Z increases. For $Z\alpha > 137$ the formation of the $j = 1/2$ states is impossible. The wavefunction inside a heavy nucleus (with finite extension) is rather different from that of a point-like charge. To avoid this problem, we take into account the finite charge distribution of the nucleus, which in principle, is not well-known. A uniform distribution gives for the potential the form,

$$U_n(r) = \begin{cases} -\frac{3Z}{2r_c} \left[1 - \frac{1}{3} \left(\frac{r}{r_c} \right)^2 \right], & 0 \leq r \leq r_c, \\ U(r), & r \geq r_c, \end{cases} \quad (13)$$

where r_c corresponds to the nuclear charge extension, and its specific value depends on the atomic system.

3.4. Rubidium atom

Two types of model potentials have been chosen for the study of Rubidium ($Z = 37$). These potentials have been used previously by Johnson et al. [13] in

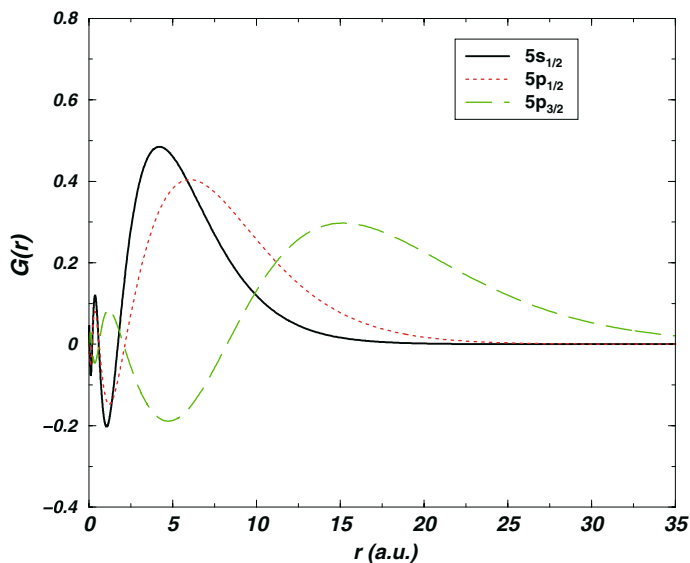


Figure 2. Rubidium radial large components for the $5s_{1/2}$, $5p_{1/2}$ and $5p_{3/2}$ eigenstates. The B-splines parameters were $n_s = 200$, $k_s = 9$, $R = 300$ a.u. and the knotpoint distribution was exponential-like.

Table 2

Green model potential, oscillator strengths for Rubidium. Core polarization effects are not taken into account. For all transitions the agreement of length-velocity forms is excellent. Experimental values (columns 2,4), taken from [14].

Rubidium, $Z = 37$, H_D						
np	$f_l(5s_{1/2} \rightarrow np_{1/2})$		$f_l(5s_{1/2} \rightarrow np_{3/2})$		$\rho \equiv f_{3/2}/f_{1/2}$	
	Green	Exp.	Green	Exp.	Green	Exp.
5	3.69(-1)	3.32(-1)	7.50(-1)	6.68(-1)	2.03	2.01
6	5.81(-3)	3.73(-3)	1.53(-2)	9.54(-3)	2.64	2.56
7	1.02(-3)	4.87(-4)	3.03(-3)	1.48(-3)	2.98	3.04
8	3.47(-4)	1.38(-4)	1.11(-3)	4.68(-4)	3.19	3.39
9	1.61(-4)	5.22(-5)	5.35(-4)	1.97(-4)	3.33	3.77
10	8.83(-5)	2.61(-5)	3.03(-4)	1.08(-4)	3.43	4.14
11	5.42(-5)	1.46(-5)	1.89(-4)	6.38(-5)	3.49	4.37
12	3.59(-5)	9.00(-6)	1.27(-4)	4.09(-5)	3.54	4.54
13	2.51(-5)	5.82(-6)	8.99(-5)	2.86(-5)	3.58	4.91
14	1.93(-5)	3.97(-6)	7.00(-5)	2.00(-5)	3.62	5.04

order to investigate P-violating electric dipole matrix elements in heavy alkali-like atoms, such as Rb, Cs, Au and Th. The specific forms of those potentials read:

Tietz:

$$U(r) = -\frac{1}{r} \left[1 + \frac{Z-1}{(1+tr)^2} \right] e^{-\gamma r}. \tag{14}$$

Green:

$$U(r) = -\frac{1}{r} \left[1 + \frac{Z-1}{H(e^{r/d} - 1) + 1} \right] e^{-\gamma r}. \quad (15)$$

where $H = d(Z-1)^{1/3}$. The parameters involved in these potentials are chosen as in the work by Johnson [13]. In figure (2) we plot the $5s_{1/2}$, $5p_{1/2}$, and $5p_{3/2}$ radial wavefunctions of Rubidium. In table (2) we give the oscillator strengths for the Rubidium from the $5s_{1/2}$ to the states $np_{1/2}$ and $np_{3/2}$ $n = 5, 6, \dots, 14$.

4. Conclusion

A numerical method is presented capable to provide accurate relativistic radial bound and continuum wavefunctions of a particle in a local central potential. The solution of the time-independent Dirac equation is approached through the finite element Galerkin method. The radial solutions are expanded in a polynomial B-spline basis, transforming the DE in a generalized eigensystem matrix problem. Comparison with the analytical solutions of the hydrogen atom is presented and applications for the non-hydrogenic atomic systems such as Rb is described. Additionally, transition dipole matrix elements and oscillator strengths between states belonging to the various partial waves are computed. Extension of the method for the calculation of multiphoton ionization cross section is straightforward.

References

- [1] H. Wabnitz et al., Nature 420 (2002) 482.
- [2] D. Xenakis et al., J. Phys. B 29 (1996) L457.
- [3] Y. Kobayashi et al., Optics Lett. 23 (1998) 64.
- [4] N.A. Papadogiannis et al., Phys. Rev. Lett. 90 (2003) 133902.
- [5] J.D. Gilaspay, J. Phys. B 34 (2001) R93.
- [6] M. Drescher et al., Nature 419 (2002) 803.
- [7] T.E.H. Walker and J.T. Waber, J. Phys. B 7 (1974) 674.
- [8] J. Colgan and M.S. Pindzola, Phys. Rev. Lett. 86 (2001) 1998.
- [9] W.R. Johnson, S.A. Blundell and J. Sapirstein, Phys. Rev. A 37 (1988) 307.
- [10] Carl de Boor, *A Practical Guide to Splines* (Springer-Verlag, New York, 1978).
- [11] Thomas Fulton and W.R. Johnson, Phys. Rev. A 34 (1986) 1686.
- [12] J. Sapirstein and W.R. Johnson, J. Phys. B 29 (1996) 5213.
- [13] W.R. Johnson et al., Phys. Rev. A 32 (1985) 2093.
- [14] L.N. Shabanova and A.N. Khlyustalov, Opt. Spectrosk (USSR) 54 (1984) 123.